Available online at www.sciencedirect.com
ScienceDirect
Bioelectrochemistry 72 (2008) 141 – 148
Bioelectrochemistry
www.elsevier.com/locate/bioelechem

Gene delivery by electroporation after dielectrophoretic positioning of cells in a non-uniform electric field

Luke A. MacQueen [a], Michael D. Buschmann [b,*], Michael R. Wertheimer [a]

[a] Department of Engineering Physics, Ecole Polytechnique, PO Box 6079 Station Centre-ville, Montreal, Qc Canada H3C 3A7
[b] Department of Chemical Engineering and Institute of Biomedical Engineering, Ecole Polytechnique, Canada

Received 5 November 2007; accepted 11 January 2008
Available online 24 January 2008

Abstract

We report the use of dielectrophoresis (DEP) to position U-937 monocytes within a non-uniform electric field, prior to electroporation (EP) for gene delivery. DEP positioning and EP pulsing were both accomplished using a common set of inert planar electrodes, micro-fabricated on a glass substrate. A single-shell model of the cell's dielectric properties and finite-element modeling of the electric field distribution permitted us to predict the major features of cell positioning. The extent to which electric pulses increased the permeability of the cell membranes to florescent molecules and to pEGFPLuc DNA plasmids were found to depend on prior positioning. For a given set of pulse parameters, EP was either irreversible (resulting in cytolysis), reversible (leading to gene delivery), or not detectable, depending on where cells were positioned. Our results clearly demonstrate that position-dependent EP of cells in a non-uniform electric field can be controlled by DEP.

Keywords: Electroporation; Electropermeabilization; Dielectrophoresis; Non-uniform electric field; Gene delivery; Transfection; Micro-electrode

1. Introduction

Biological cells of various types can be distinguished from one-another and displaced within a liquid medium using dielectrophoresis (DEP) [1]. In a spatially non-uniform electric field, E, the differential electric polarizability of cells and their suspending medium produces the DEP force, which can be either attractive (towards the strong-E regions) or repulsive (towards the weak-E regions), depending on experimental conditions. Attractive or repulsive DEP forces are usually referred to as "positive" (pDEP) or "negative" (nDEP), respectively. Measurement of the DEP force as a function of experimental variables produces DEP "spectra" which are characteristic of each cell-type, allowing for cell separation and identification [2,3]. In microfluidic devices, DEP has been used to transport and position cells with sufficient precision to enable single-cell manipulation [4–6].

Microfluidic devices for single-cell or sub-cellular analysis often use electric field-based techniques other than DEP to increase permeability of the cell membrane [7–9], or to induce cytolysis [10,11]: Electroporation or electropermeabilization (EP) results from the application of an intense electric field to bring about structural changes of the cell membrane that increase its permeability. It is well known that irreversible EP leads to cytolysis [12], while reversible EP can be used to transfer molecules such as DNA into the cells while maintaining high rates of cell survival [13]. Generally, pulsed electric fields are used and the extent of EP is determined by parameters such as the strength, duration, and repetition rate of the electric pulses. Critical values of the electric field strength, which determine whether cell membrane EP is reversible or irreversible, are specific to each cell-type and are usually determined by performing experiments at different E values [14,15].

Traditionally, *in vitro* EP has been accomplished using electrodes with millimeter spacing, and the position of individual

* Corresponding author. Tel.: +1 514 340 4711x4931; fax: +1 514 340 2980.
E-mail address: michael.buschmann@polymtl.ca (M.D. Buschmann).
URL: http://www.polymtl.ca/tissue/ (M.D. Buschmann).

1567-5394/$ - see front matter © 2008 Elsevier B.V. All rights reserved.
doi:10.1016/j.bioelechem.2008.01.006

cells within the electrode chamber did not need to be considered [16]. In contrast, micro-fabricated devices for EP accommodate relatively small numbers of cells and their smaller (sub-mm) electrode dimensions require consideration of spatial non-uniformities in E and of cell positioning with respect to the electrodes [7–11]. Cell positioning by DEP is known to complement EP experiments. For example, the alignment of cells by DEP after EP has been used for cell–cell fusion [17], and EP of DEP-trapped cells increased the sensitivity of impedance-based cell-detection [18]. In a spatially non-uniform E, the dependence of EP on the field's amplitude results in position-dependent EP, and therefore leads to regions within the chamber where either reversible or irreversible EP may prevail [19,20].

In the present report, we have used spatially non-uniform E to assess the extent of reversible and irreversible EP as a function of cell position within the electrode chamber. As a first step, position-dependent EP of a single cell-type, U-937 [21], was investigated using florescent probes. We selected a single cell-type to ensure that pulsing conditions required for EP were similar for all cells, such that any differences in EP would primarily be due to their positioning. We then used DEP to accentuate position-dependent EP, by moving cells into specific regions within the electrode chamber. Gene delivery was accomplished for all cases of cells being randomly distributed, or selectively positioned by DEP prior to EP, however the number of successfully transfected cells and their viability depended on the specific conditions of EP and of DEP.

2. Methodologies

2.1. DEP analyses using a single-shell dielectric model of a spherical cell

Dielectric parameters were determined independently of EP experiments, by fitting the measured cross-over frequency from DEP experiments (defined in Eq. (3) below) with a single-shell model of the spherical cell [22,23]. Different values of the complex electrical permittivity, ε^*, were assigned to the external medium, $\varepsilon_e^*=\varepsilon_e-j\sigma_e/\omega$, to the cell membrane, $\varepsilon_m^*=\varepsilon_m-j\sigma_m/\omega$, and to the (internal) cytosol, $\varepsilon_i^*=\varepsilon_i-j\sigma_i/\omega$, where ε designates permittivity, σ electrical conductivity, and $\omega=2\pi f$ angular frequency, f being the frequency of the applied sinusoidal electric field, and $j=\sqrt{-1}$. The *relative* permittivity is $\kappa=\varepsilon/\varepsilon_0$, ε_0 being the permittivity of free space.

The DEP phenomena observed in the present work can be modeled using the following four equations (Eqs. (1)–(4)) [25]: The DEP force, F_{DEP}, for the case of a spherical cell of radius, a, is approximated by

$$F_{DEP}=2\pi\varepsilon_e a^3 Re[K(\omega)]\nabla E^2, \tag{1}$$

where the polarization factor, K, is

$$K(\omega)=\frac{\varepsilon_{cell}^*-\varepsilon_e^*}{n\varepsilon_{cell}^*+(n+1)\varepsilon_e^*}, \tag{2}$$

where $\varepsilon_{cell}^*=\varepsilon_{cell}-j\sigma_{cell}/\omega$ is the complex electrical permittivity of the cell and n is the multipolar term (for the present spherical case, we assumed a pure dipole, $n=1$). nDEP and pDEP correspond to $K<0$ and $K>0$, respectively. A single "cross-over" frequency, f_0, defined by $K(f_0)=0$ and $F_{DEP}(f_0)=0$, was seen in DEP experiments (described below) when $f<10^7$ Hz:

$$f_0=\frac{1}{2\pi}\left(\frac{(\sigma_e-\sigma_{cell})(\sigma_{cell}+2\sigma_e)}{(\varepsilon_{cell}-\varepsilon_e)(\varepsilon_{cell}+2\varepsilon_e)}\right)^{\frac{1}{2}} \tag{3}$$

The effective complex permittivity of the cell, ε_{cell}^*, based on the above single-shell theory is

$$\varepsilon_{cell}^*=\varepsilon_m^*\frac{\left(\frac{a}{a-d}\right)^3+2\frac{\varepsilon_i^*-\varepsilon_m^*}{\varepsilon_i^*+2\varepsilon_m^*}}{\left(\frac{a}{a-d}\right)^3-\frac{\varepsilon_i^*-\varepsilon_m^*}{\varepsilon_i^*+2\varepsilon_m^*}}, \tag{4}$$

where d is the membrane's thickness. This model has been used in previous work to measure ε_m^*, ε_i^* and the area-specific conductance of the membrane, $G_m=\sigma_m/d$, for several cell-types, using DEP [2,3,22,23] and the electrorotation technique [24,26,27]. In our study we took fixed values for a, d, σ_m, ε_i and ε_e. We assumed $a=7.5$ μm (from optical measurements), $d=7$ nm [27], $\sigma_m=10^{-6}$ S m^{-1}, and $\varepsilon_i=\varepsilon_e=80\varepsilon_0$, as will be further discussed below. The experimental conditions determined f and σ_e, that were in the ranges $10^4<f(\text{Hz})<10^7$ and $10^{-3}<\sigma_e$ (S m^{-1}) <1.6. The remaining two parameters, ε_m and σ_i, were then found by fitting experimental f_0 data using Eq. (2) ($K(f_0)=0$), with ε_{cell}^* given by Eq. (4) and restricting the fit parameters to the ranges $0.2<\sigma_i$ (S m^{-1}) <1; and $3\varepsilon_0<\varepsilon_m<23\varepsilon_0$. The differences between measured and calculated values of f_0 were minimized using a least-squares algorithm (lsqcurvefit, Matlab v. 7.2, The Mathworks, Natick, MA).

The polarization factor $K(f,\sigma_e)$ determines cell positioning by DEP, where nDEP occurs when K(low-f) <0 and pDEP when K (high-f) >0. Using parameters found from best fits presented below in the results ($\varepsilon_m=6.0\varepsilon_0$, $\sigma_i=0.425$ S m^{-1}), the cross-over frequency, f_0, is seen to increase when σ_e increases (from A to B to C to D in Fig. 1). When $\sigma_e>>\sigma_i$, $K<0$ for all values of f, and only nDEP can occur (Fig. 1, curves C and D).

2.2. Fabrication of electrodes and modeling of the electric field

Planar Ti/Pt electrodes were fabricated on glass substrates using standard lift-off processes [28]: Chromium masks were

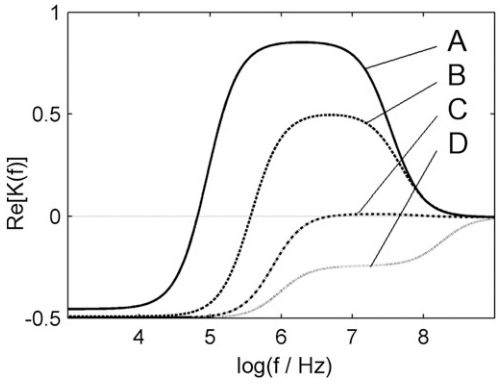

Fig. 1. The real part of the polarization factor, $Re[K(f)]$, in Eqs. (1) and (2) versus frequency, f, for model parameters corresponding to U-937 monocytes and at different values of σ_e. A: $\sigma_e=0.0175$ S m^{-1}; B: $\sigma_e=0.1$ S m^{-1}; C: $\sigma_e=0.4$ S m^{-1}; and D: $\sigma_e=1.0$ S m^{-1}.

fabricated on glass (Bandwidth Foundry, Sydney, NSW, Australia) and photolithography was carried out by spin-coating an adhesion promoter, AP300 (Silicon Resources, Chandler, AZ), a lift-off resist LOR5A (MicroChem, Newton, MA) and a final, positive, resist S1813 (Shipley, now part of Rohm & Haas, Philadelphia, PA). UV exposure was done using a Karl Süss MA-4 mask aligner (Süss Microtec, Waterbury Center, VT). The electrodes were deposited by electron beam evaporation (Ti adhesion layer, 10 nm) and sputtering (Pt layer, 70 nm), the former under ultra-high-vacuum and the latter in Argon at 2.4 Pa. For each glass slide (dimensions: 76.2×25.4×1.5 mm), the lift-off procedure produced 12 sets of electrodes, each with three leads (Fig. 2a) to which electrical connectors were bonded using a combination of conductive silver epoxy (MG Chemicals, Surrey, BC, Canada) and a standard two-phase epoxy (LePage, Toronto, ON, Canada). The electrodes were placed within the microscope slide-carrier of an inverted optical microscope (AxioVert S100TV, Carl Zeiss Microimaging, Thornwood, NY) and connected to a signal generator (Model 33220A, Agilent, Palo Alto, CA), which was used to generate both sine waves for DEP and square pulses for EP, without the requirement for any additional signal conditioning or amplification. During DEP manipulations, the central electrode was driven at opposite polarity to the surrounding structure (Fig. 2b, e2 and e1, respectively). The latter possessed periodically-spaced triangular features, which gave rise to alternating regions of strong- and weak-E (Fig. 2c). The electrode area over which significant DEP occurred (Fig. 2c, outlined trace) was about 3 mm^2. The distance of closest approach between the inner two electrodes (at the tip of each triangular portion) was 50 μm.

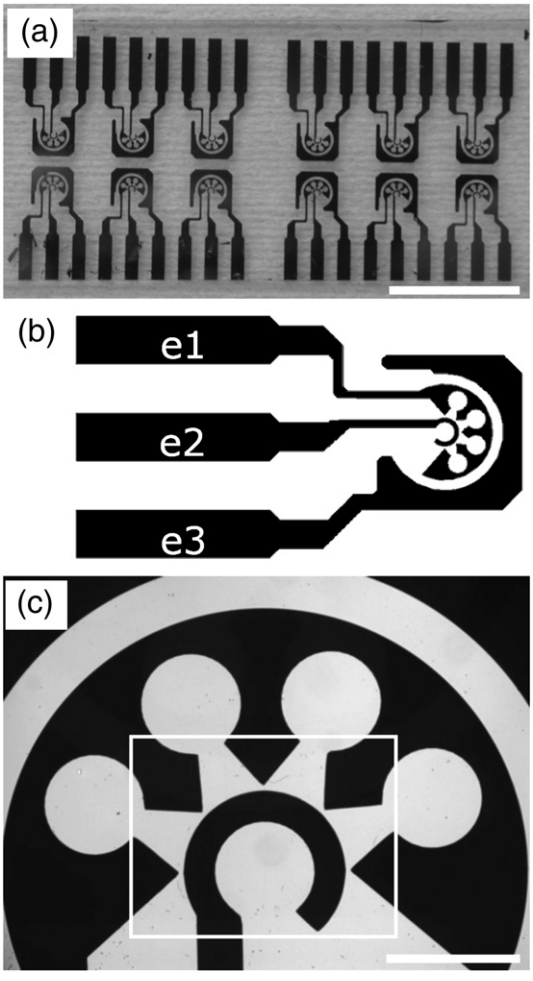

Fig. 2. Ti/Pt electrodes deposited on a glass microscope slide. (a) Twelve sets of 3-lead electrodes. Scale bar is 1.5 cm. (b) One 3-lead electrode set with electrodes labeled e1, e2, and e3. The inner two electrodes, e1 and e2, are driven at opposite polarity, while the outermost electrode, e3, is grounded. (c) Magnified view of the inner two electrodes, e1 and e2. The rectangular trace represents the region used for DEP: Strong- and weak-E regions occur where e1 approaches and recedes from e2, respectively. Scale bar is 1 mm.

We defined positions within 50 μm of the electrode edges as strong-E regions, and otherwise as weak-E. The values of E averaged over the strong and weak regions differed by a factor of approximately three. For example, when the applied voltage was $U=10$ V, the maximum value of $E=U/l$, where l is the inter-electrode distance, was 200 kV m^{-1}. The E values averaged over the strong- and weak-E regions were ~180 kV m^{-1} and ~60 kV m^{-1}, respectively. These estimates of E were accomplished with Comsol Multiphysics v3.2 software (Comsol, Stockholm, Sweden) using the conductive media mode with the electric potential assigned at boundaries (Dirichlet-type of boundary conditions), and assuming a homogeneous medium in which the presence of cells was neglected.

2.3. Cells and media

An established human monocytic cell-line, U-937, obtained from ATCC (Manassas, VA), was chosen for these experiments, primarily because these cells are cultured in suspension and tend not to adhere either to solid surfaces or to one-another. The cells were cultured in RPMI 1640 (Sigma-Aldrich, St. Louis, MO) supplemented with 10% FBS (Atlanta Biologicals, Laurenceville, GA), and incubated at 37 °C in an atmosphere supplemented with 5% CO_2. Prior to EP and DEP experiments, the cells were centrifuged at 190 g for 5 min (Model CR4 22, Jouan, Saint-Herblain, France) and re-suspended in one of several low-conductivity buffers. Buffers of different conductivity were made by diluting phosphate-buffered saline (PBS D1283: 136.8 mM NaCl, 8.1 mM Na_2HPO_4, 2.7 mM KCl, 1.5 mM KH_2PO_4, Sigma) in de-ionized water (DI-H_2O), and adding D-glucose (Sigma) to maintain the osmolality at 200±25 mOsm kg^{-1} (close to the isotonic value of~285 mOsm kg^{-1}). A slightly hypotonic buffer was used to induce a slight swelling of the cells that is advantageous for EP experiments since the amplitude and numbers of pulses could be reduced compared to the isotonic case [29,30]. The cell radius (and standard deviation) was estimated at $a=7.5\pm1.0$ μm, on using the straight-line measurement feature of imaging software (Northern Eclipse v. 7.0, Empix Imaging, Mississauga, ON, Canada). In comparison, the isotonic value was $a=6.25\pm1.0$ μm. This level of hypotonicity was considered acceptable with reference to the relatively large range of osmolalities 75<Osmolality (mOsm kg^{-1})<300 used in previous EP-based experiments [29,30]. The pH was always above 6.0±0.5, and was also safe for short-term use, cells being kept within the buffer solution for less than 15 min. The conductivity range of the diluted PBS buffers

was $10^{-3} < \sigma_e$ (S m^{-1}) < 1.6, and the maximum concentration of D-glucose required, corresponding to the medium with lowest σ_e, was 220 mM. Conductivity and pH were measured using an Accumet model 20 instrument (Fisher Scientific, Hampton, NH), and osmolality was measured using a model 3D3 osmometer, based on freezing-point depression (Advanced Instruments, Norwood, MA).

2.4. Cell positioning and measurement of the cross-over frequency

Unless otherwise stated, cells were suspended in buffer at a density of $\sim 5 \times 10^5$ cells mL^{-1}, as measured by hemocytometer (VWR Scientific, Mississauga ON), and were transferred in 7.5 μL volumes to the electrode surface using a micropipette. This produced a ~250 μm deep liquid layer containing ~3750 cells, which covered an area of ~30 mm^2. The DEP signal applied to the electrodes was a sine wave with a peak voltage of $U = 3$ V, and a frequency sweep $10^4 < f$ (Hz) $< 10^7$ was performed for each value of σ_e. Cell behavior was monitored visually or with a CCD camera (Model QIC-F-/M2: QImaging, Burnaby, BC, Canada), and still images were captured for subsequent analysis. Under these conditions, the majority of cells attained equilibrium positions along the plane of the electrodes after about 5 min, by a combination of DEP and sedimentation, at which point the experiment was stopped. Cell positioning statistics were then compiled from the image by counting the cells that had migrated to strong-E regions (where the distance between cells and electrode edges was <50 μm), versus weak-E regions (where the distance between cells and electrode edges was >50 μm).

Under certain conditions with appropriate choices of f and σ_e, F_{DEP} was found to be negligible, and cells remained randomly distributed over the electrode surfaces. As described above, the corresponding f values are the "cross-over" frequencies, f_0, and a different value of f_0 was found for each value of σ_e. To determine f_0, we repeated the positioning experiments at different f values, until random distributions of cells were observed, approaching f_0 from frequencies both above and below f_0 in order to minimize error. This procedure was repeated three times for each σ_e.

2.5. Electroporation and gene delivery

We used square-wave bipolar electric pulses for electroporation. For each experimental condition, a sequence of six pulses was applied, each with width $t_e = 20$ μs, rise- and fall times of $t_s = 5$ ns, and inter-pulse intervals $t_r = 0.5$ s (that is, repetition rate, rr = 2 Hz). Peak applied voltages were $U = 7$, 8, 9, and 10 V. First, randomly distributed cells were electroporated in the presence of fluorescent probes, to visualize the spatial dependence of EP in the case of a non-uniform electric field. Cell positioning by DEP was used to accentuate this position-dependence of EP and further influence gene transfer. Expression of the transferred genes and cell viability (cell survival) were quantified by determining the ratios N_T/N_{TOT} and N_S/N_{TOT}, N_T being the number of transfected cells, N_S the number of surviving cells, and N_{TOT} the total number of cells.

We used a "Live(green)/Dead(red)" cytotoxicity kit (Invitrogen, Carlsbad, CA) to visualize the position-dependence of EP. The protocol consists of adding a mixture of two different fluorescent indicators, each at 1 μM concentration, to the cell suspension. The first indicator, Calcein AM, can enter through the cell membrane and then be cleaved by esterases in healthy cells to become fluorescent (green). The second indicator, Ethidium HD-1, is excluded from healthy cells with intact cell membranes, but traverses those that have been compromised; once inside the nucleus, it binds to nucleic acids, which greatly (40×) increases its fluorescence (red). Thus, healthy cells appear green, irreversibly damaged cells red, and reversibly electroporated cells appear orange due to the combined presence of both indicators. Live/Dead EP results were obtained using a random and uniform distribution of cells to assess position-dependence of EP due to the spatially varying E.

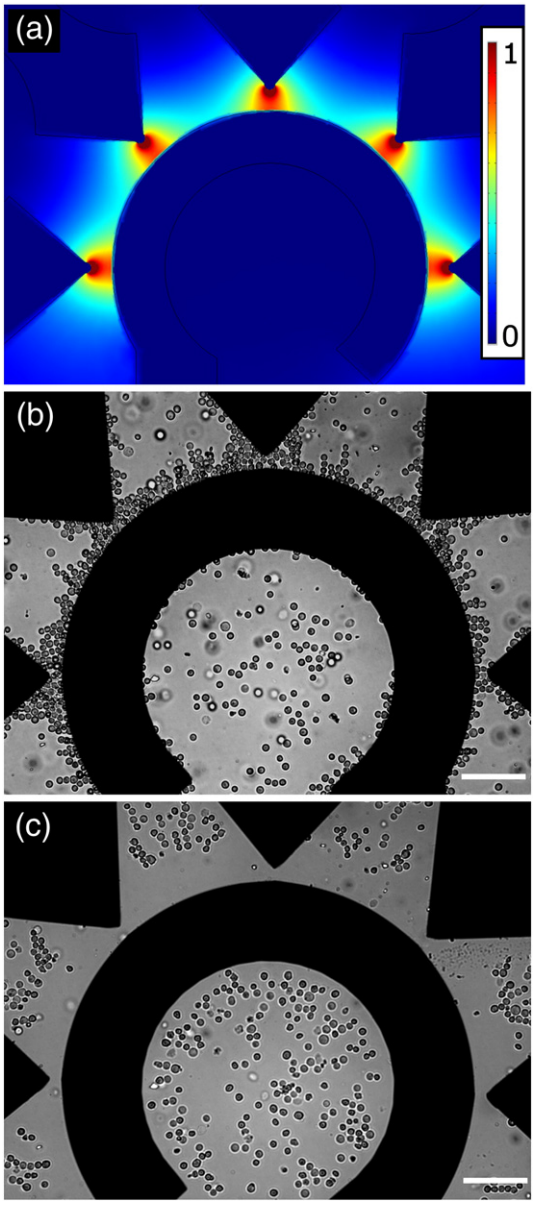

Fig. 3. Positioning of U-937 monocytes by DEP. (a) Simulated electric field distribution using an arbitrary linear scale. (b) Cells positioned in the strong-E regions by pDEP. (c) Cells positioned in the weak-E regions by nDEP. Scale bars are 300 μm.

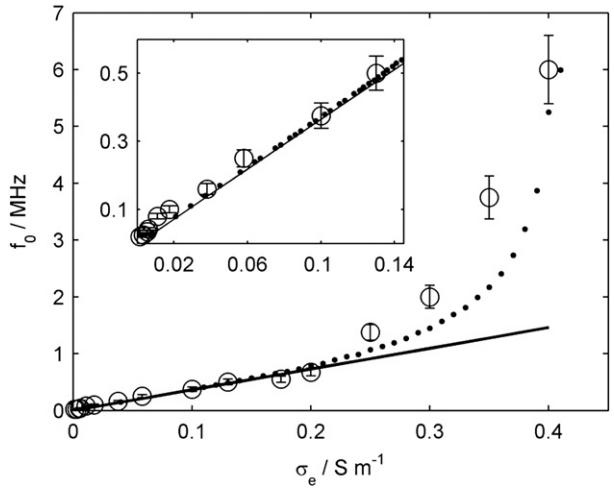

Fig. 4. The cross-over frequency, f_0, versus conductivity of the extracellular medium, σ_e, for U-937 monocytes. Open circles are experimental f_0 (mean ± SD, $n=3$), while the dotted line is a fit using Eqs. (2) and (4), and the solid line is a fit using Eq. (3). The inset shows the region of low σ_e.

For gene transfer we used a DNA plasmid expressing a fluorescent reporter, pEGFPLuc (Clontech, Mountain View CA), at a concentration of 0.55 μg mL^{-1}. As above, 7.5 μL of buffer containing cells and DNA were placed over the electrodes at a cell density of $D=5\times10^5$ cells mL^{-1} (total number of cells ~3750). The buffer was PBS diluted in DI-H_2O, with conductivity $\sigma_e=$ 50 mS m^{-1}, and osmolality = 200 ± 25 mOsm kg^{-1}. Transfection experiments were performed at room temperature (27 °C, or 300 K) under four sets of conditions: (i) EP pulses were applied after the cells had been positioned by pDEP for 5 min, using a 3 V, 1 MHz sinusoidal potential; (ii) EP pulses were applied after 5 min of nDEP positioning, using a 3 V, 40 kHz sinusoidal potential; (iii) EP pulses were applied after 5 min of sedimentation only ("no DEP"); and (iv) as a control with neither DEP nor EP pulses. Each condition (i) to (iv) was repeated four times. Following gene transfer, cells were incubated in FBS-supplemented RPMI growth medium at 37 °C with 5% CO_2. The number of transfected cells, N_T, and surviving cells, N_S, were monitored by fluorescence microscopy.

3. Results

3.1. Cell positioning

The measured DEP spectra of cells reveal the ranges of f and σ_e for which both pDEP and nDEP positioning were achieved (Fig. 3b and c, respectively). The data can be represented by the cross-over frequencies (Fig. 4), where a linear relationship between f_0 and σ_e was observed for $0.02<\sigma_e$ (S m^{-1}) <0.2. When σ_e was close to physiological (1.5 S m^{-1}), only nDEP was observed within the frequency range investigated, the onset of pDEP occurring only when $\sigma_e<0.4$ S m^{-1}. The intercept of f_0 data extrapolated towards $\sigma_e=0$ (the origin in Fig. 4) was close enough to zero that an upper limit of $\sigma_m<10^{-5}$ S m^{-1} ($G_m<1430$ S m^{-2}) could be determined. These small values of σ_m have a negligible effect when calculating K, for $\sigma_e>5\times10^{-2}$ S m^{-1} so that we assumed $\sigma_m=10^{-6}$ S m^{-1} for further calculations and for model fitting.

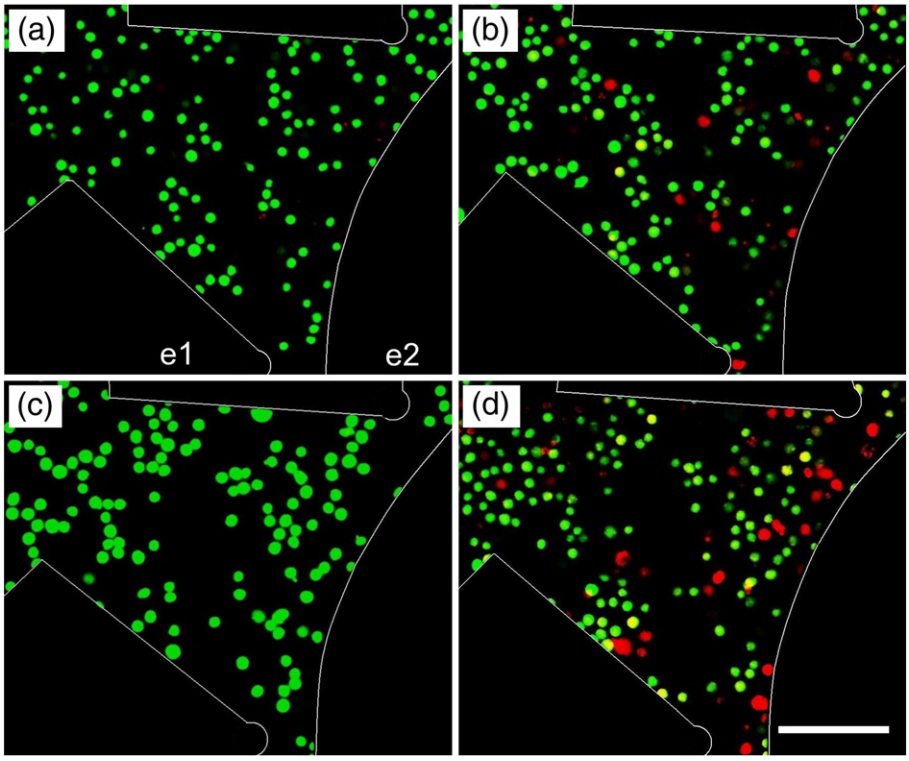

Fig. 5. Position-dependent EP of U-937 monocytes, as monitored by "Live(green)/Dead(red)" florescence tests. (a) Live cells, shown before pulsing. (b) The same cells shown in (a), but 5 min after applying pulses of amplitude $U=8$ V, showing limited cell death. (c) Live cells shown before pulsing. (d) The same cells shown in (c), but 5 min after applying pulses of amplitude $U=10$ V, showing more extensive cell death near the pDEP region. Electrode (e1, e2) edges are outlined for clarity. Scale bar is 100 μm.

We fit f_0 data to both Eq. (2) (with the condition $K(f_0)=0$) and Eq. (3) (valid for $\sigma_e < \sim 0.2$ S m^{-1}, see Fig. 4) by varying ε_m and σ_i, with other parameters fixed at $a=7.5$ μm, $d=7.0$ nm, $\sigma_m = 10^{-6}$ S m^{-1} and $\varepsilon_i=\varepsilon_e=80\varepsilon_0$. The best fit for both equations was found when $\varepsilon_m=6.0\varepsilon_0$ ($C_m=7.6$ mF m^{-2}) and $\sigma_i=0.425$ S m^{-1}. These data therefore provide estimates for the dielectric properties of U-937 monocytes as $\sigma_m < 10^{-5}$ S m^{-1} ($G_m < 1430$ S m^{-2}), $\varepsilon_m = 6.0\varepsilon_0$ ($C_m = 7.6 \pm 1.25$ mF m^{-2}), $\sigma_i=0.425$ S m^{-1}, and $\varepsilon_i=80\varepsilon_0$, and can be used to predict DEP responses under arbitrary conditions of f and σ_e.

3.2. Live/Dead viability tests

During DEP experiments with $U<4$ V, Live/Dead tests revealed that the U-937 cells remained viable for at least 15 min, independent of f and σ_e values. Thus an amplitude of $U=3$ V was used for subsequent DEP positioning prior to EP.

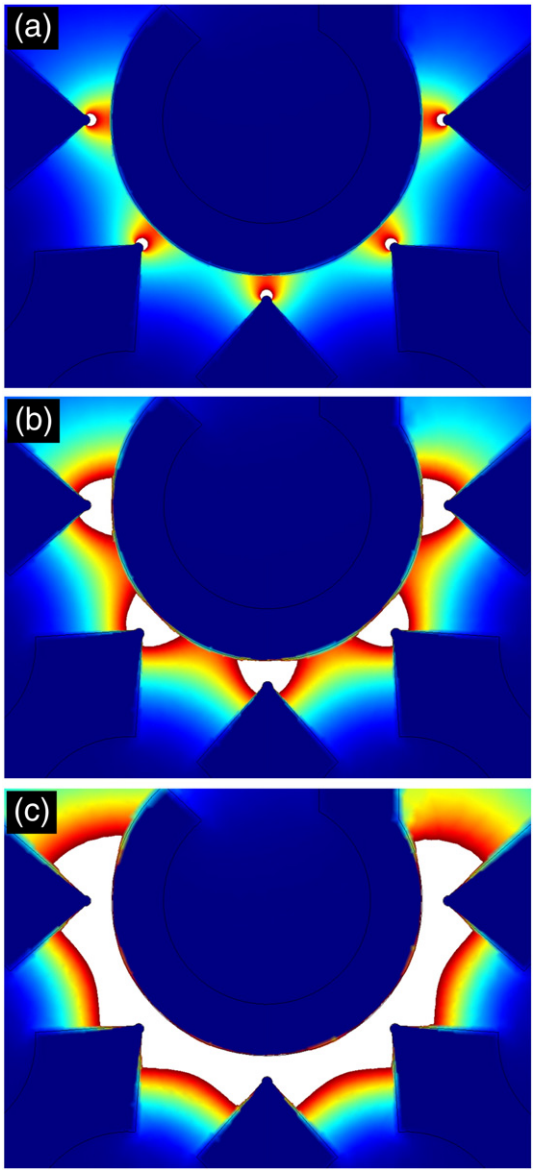

Fig. 6. Calculated position-dependence of EP of U-937 monocytes, for different values of U. White = irreversible EP (cytolysis), Red-Green = reversible EP, Blue = no EP. (a) $U=6$ V, (b) $U=8$ V, (c) $U=10$ V.

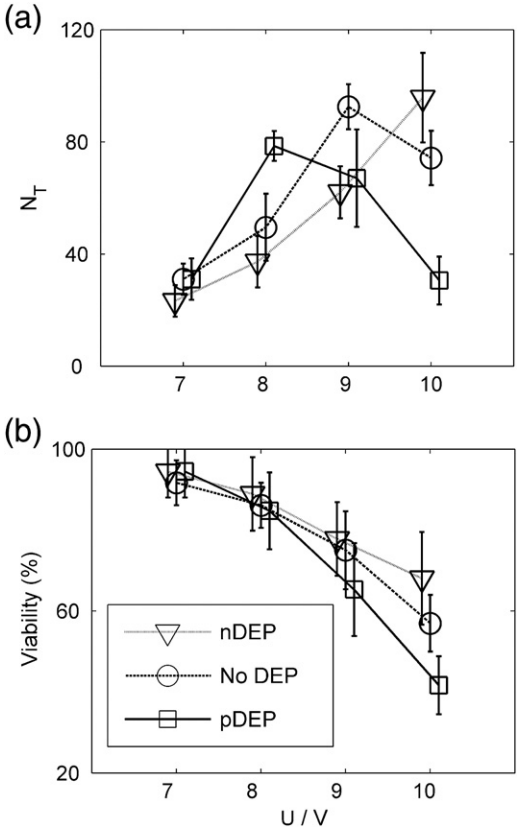

Fig. 7. Position-dependent gene transfection level and viability of U-937 monocytes. (a) Number of transfected cells, N_T, and (b) viability versus pulse amplitude, U, for cells positioned by either pDEP (squares), nDEP (triangles), or with "no DEP" (no induced positioning, circles) prior to pulsing. Mean±SD ($n=4$) values are shown, and data were shifted slightly to increase clarity between groups.

The application of higher voltage (7 V$<U<$10 V), short-duration ($t_e < 100$ μs) pulses demonstrated position-dependent EP within the region of spatially non-uniform electric field. Although cells displayed some heterogeneous behaviour (some cells in the strong-E regions remained green, while others in weak-E regions became red), a clear position-dependent response to EP could be observed (Fig. 5), consistent with the calculated distribution of E (Fig. 6). For the case of low pulse amplitudes ($U<4$ V), few green-to-red transitions occurred (less than 3% of cells), but as U was increased the regions containing red cells expanded from the tips of the "e1" electrodes to eventually fill in the space between electrodes e1 and e2 when $U>8$ V (Figs. 5d and 6c). Therefore, the "critical" field values for reversible and irreversible EP could be estimated from calculated field values and these cell distributions as $E=40$ kV m^{-1} and $E=120$ kV m^{-1}, respectively. For example, when $U=10$ V, the region of irreversible EP coincided with that in which pDEP was observed in the course of cell positioning experiments (Fig. 3b), while reversible EP was observed in the nDEP region (Fig. 3c).

3.3. Gene delivery

Cell positioning by DEP prior to EP significantly influences transfection efficiency and cell viability, compared with randomly

distributed cells ("no DEP") under otherwise identical pulsing conditions (Fig. 7). For EP amplitudes of $U=7$ or 8 V, viability was generally high, while higher EP amplitudes reduced viability (Fig. 7b). A coupling between DEP and EP was evident, where the number of transfected cells increased with U initially for all three cases (nDEP, no DEP, pDEP) (Fig. 7a), but then decreased above $U=8$ V, initially for pDEP and then for "no DEP". Cell viability decreased monotonically as EP amplitude U increased. Transfected cells that survived the first 24 h after EP remained viable and were observed to proliferate for the duration of our observations (one week). For the control group (no DEP, no pulses) we found $N_T=0$, as expected.

It is important to note that a sizeable fraction of cells remained outside the DEP/EP-affected regions (identified in Fig. 2c), and that these cells were later counted when compiling transfection data (Fig. 7). This was the result of the necessarily quite large (7.5 μL) volumes of cell suspension applied, and led to a relatively high background of viable but non-transfectable cells that were estimated to be ~30% of the total cell number.

4. Discussion

4.1. Dielectrophoresis and electroporation

The major features of DEP positioning were adequately predicted using a single-shell theory, with static dielectric properties of the membrane, (ε_m, σ_m), cytosol, (ε_i, σ_i), and media (ε_e, σ_e). Best fit values of $\varepsilon_m=6.0\varepsilon_0$ ($C_m=7.6\pm1.25$ mF m^{-2}), $\sigma_m<10^{-5}$ S m^{-1} ($G_m<1430$ S m^{-2}), and $\sigma_i=0.425$ S m^{-1}, with ε_i taken as $80\varepsilon_0$, are comparable to previously published parameters for U-937 monocytes [3], particularly when the low osmolarity is taken into account [29]. The measurements of f_0 allowed optimization of experimental parameters (ranges of f and σ_e values), in order to examine the influence of cell positioning by DEP on cell transfection.

We found that the spatial non-uniformity of E used during DEP produced a position-dependent EP. Comparing cell positioning by DEP (Fig. 3) with the position-dependence of EP for randomly distributed cells (Fig. 5) reveals how pDEP and nDEP increased and decreased, respectively, the EP and number of transfected cells. For a given value of U, the field acting on cells in the strong-E region (corresponding to pDEP) was, on average, three times higher than in the weak-E region (corresponding to nDEP). Thus, for example, when $U=8$ V, the average E in the nDEP region was too low for significant EP, in contrast to the pDEP region. In the case of still higher U ($U>8$ V), lysis of cells frequently occurred in the pDEP region, resulting in low viability and low N_T (Fig. 7) while nDEP positioned cells retained better viability and increased transfection efficiency.

The occurrence of "optimal" E values, the range below which transfection is low and above which viability drops, is well known in the literature [14,15]. Generally, when E is spatially uniform, experiments designed to correlate EP with field strength are repeated at different U values. The present spatially non-uniform field offers an advantage that for a given U and set of pulse conditions (fixed values of t_e, t_r, and t_s), EP can be visualised for a range of E in a single experiment. For the present conditions and cell-type, we estimated "critical" field strengths of $E=40$ kV m^{-1} for reversible EP, and $E=120$ kV m^{-1} for irreversible EP. Therefore, reversible EP leading to the possible uptake of dyes and genes was observed to occur in the range $40<E$ (kV m^{-1}) <120. Since the regions within the electrode chamber where these conditions existed could be calculated from U, we were able to predict the extent of EP-based on the combined effect of DEP cell positioning and the EP pulse amplitude U.

4.2. Limitations

Commercial electroporators are capable of transfecting various cell-types (including U-937) with a higher efficiency than that reported here. This is in part due to the fact that the device presented here allows ~30% of cells to remain in low-E regions, and they were therefore not transfected. Additionally, we did not optimize the cell transfection medium with special reagents that are used in commercial systems. Another limitation related to prediction of gene transfer is the use of the Live/Dead viability tests with dyes that are ~4200 times smaller (by molecular weight) than the DNA plasmid.

5. Conclusions

Several new micro-devices for the manipulation of biological cells have been reported in the literature. Dielectrophoresis (DEP) and electroporation (EP) enable diverse manipulations such as physical displacement (transport and trapping of cells), and gene delivery. The present simple planar micro-electrode device demonstrated that applying both DEP and EP in a spatially non-uniform electric field, permitted correlation of EP with electric field strength. Regions within the electrode chamber where reversible or irreversible EP occurred could then be predicted by the choice of EP pulse height U, and DEP positioning allowed additional control over the outcome of EP. This study shows that future devices may combine DEP and EP using spatially non-uniform fields to achieve different objectives in cell movement and manipulation.

Acknowledgements

This work was supported by the Natural Sciences and Engineering Research Council of Canada (NSERC), and by the Canadian Institutes of Health Research (CIHR). The authors thank Yves Drolet for his technical assistance, and Drs. Stéphane Methot and Marc Lavertu for providing the pEGFP plasmids. We also thank the staff of the Micro-fabrication Laboratories (LMF) for their help and expertise, in particular Dr. Souleymane Bah for his assistance with photolithography and fabrication of electrodes.

References

[1] H.A. Pohl, Dielectrophoresis, Cambridge University Press, Cambridge, UK, 1978.
[2] F.F. Becker, X.-B. Wang, Y. Huang, R. Pethig, J. Vykoukal, P.R.C. Gascoyne, Separation of human breast cancer cells from blood by differential dielectric affinity, Proc. Natl. Acad. Sci. USA 92 (1995) 860–864.

[3] Y. Huang, S. Joo, M. Duhon, M. Heller, B. Wallace, X. Xu, Dielectrophoretic cell separation and gene expression profiling on microelectronic chip arrays, Anal. Chem. 74 (2002) 3362–3371.
[4] J. Suehiro, R. Pethig, The dielectrophoretic movement and positioning of a biological cell using a three-dimensional grid electrode system, J. Phys. D: Appl. Phys. 31 (1998) 3298–3305.
[5] T. Müller, G. Gradl, S. Howitz, S. Shirley, Th. Schnelle, G. Fuhr, A 3-D microelectrode system for handling and caging single cells and particles, Biosens. Bioelectron. 14 (1999) 247–256.
[6] A. Rosenthal, B.M. Taff, J. Voldman, Quantitative modeling of dielectrophoretic traps, Lab. Chip 6 (2006) 508–515.
[7] J.A. Lundqvist, F. Sahlin, M.A. Aberg, A. Stromberg, P.S. Eriksson, O. Orwar, Altering the biochemical state of individual cultured cells and organelles with ultramicroelectrodes, Proc. Natl. Acad. Sci. USA 95 (1998) 10356–10360.
[8] M. Khine, A. Lau, C. Ionescu-Zanetti, J. Seo, L.P. Lee, A single cell electroporation chip, Lab. Chip 5 (2005) 38–43.
[9] M.B. Fox, D.C. Esveld, A. Valero, R. Luttge, H.C. Mastwijk, P.V. Bartels, A. van den Berg, R.M. Boom, Electroporation of cells in microfluidic devices: a review, Anal. Bioanal. Chem. 385 (2006) 474–485.
[10] S.-W. Lee, Y.-C. Tai, A micro cell lysis device, Sens. Actuators A: Phys. 73 (1999) 74–79.
[11] M.A. McClain, C.T. Culbertson, S.C. Jacobson, N.L. Allbritton, C.E. Sims, J.M. Ramsey, Microfluidic devices for the high-throughput chemical analysis of cells, Anal. Chem. 75 (2003) 5646–5655.
[12] A.J.H. Sale, W.A. Hamilton, Effects of high electric fields on microorganisms, Biochem. Biophys. Acta 148/3 (1967) 781–788.
[13] E. Neumann, M. Schaefer-Ridder, Y. Wang, P.H. Hofschneider, Gene transfer into mouse lyoma cells by electroporation in high electric fields, EMBO 1 (1982) 841–845.
[14] E. Neumann, The relaxation hysteresis of membrane electroporation, in: A.E. Sowers, C.A. Jordan (Eds.), Electroporation and Electrofusion in Cell Biology, Plenum Press, New York, 1989.
[15] T. Kotnik, L.M. Mir, K. Flisar, M. Puc, D. Miklavčič, Cell membrane electropermeabilization by symmetrical bipolar rectangular pulses: part 1. Increased efficiency of permeabilization, Bioelectrochemistry 54 (2001) 83–90.
[16] M. Puc, S. Čorović, K. Flisar, M. Petkovšek, J. Nastran, D. Miklavčič, Techniques of signal generation required for electropermeabilization. Survey of electropermeabilization devices, Bioelectrochemistry 64 (2004) 113–124.
[17] U. Zimmermann, Electric field-mediated fusion and related electrical phenomena, Biochem. Biophys. Acta 694/3 (1982) 227–277.
[18] J. Suehiro, T. Hatano, M. Shutou, M. Hara, Improvement of electric pulse shape for electropermeabilization-assisted dielectrophoretic impedance measurement for high sensitive bacteria detection, Sens. Actuators B: Chem. 109 (2005) 209–215.
[19] T. Heida, J.B.M. Wagenaar, W.L.C. Rutten, E. Marani, Investigating membrane breakdown of neuronal cells exposed to nonuniform electric fields by finite-element modeling and experiments, IEEE Trans. Biomed. Eng. 49 (2002) 1195–1203.
[20] T.R. Gowrishankar, D.A. Stewart, J.C. Weaver, Model of a confined spherical cell in uniform and heterogeneous applied electric fields, Bioelectrochemistry 68 (2006) 181–190.
[21] C. Sundstrom, K. Nilsson, Establishment and characterization of a human histiocytic lymphoma cell line (U-937), Int. J. Cancer 17 (1976) 565–577.
[22] P. Gascoyne, R. Pethig, J. Satayavivad, F.F. Becker, M. Ruchirawat, Dielectrophoretic detection of changes in erythrocyte membranes following malarial infection, Biochim. Biophys. Acta 1323 (1997) 240–252.
[23] F.H. Labeed, H.M. Coley, H. Thomas, M.P. Hughes, Assessment of multidrug resistance reversal using dielectrophoresis and flow cytometry, Biophys. J. 85 (2003) 2028–2034.
[24] X. Hu, W.M. Arnold, U. Zimmermann, Alterations in the electrical properties of T and B lymphocyte membranes induced by mitogenic stimulation. Activation monitored by electro-rotation of single cells, Biochim. Biophys. Acta 1021 (1990) 191–200.
[25] T.B. Jones, Electromechanics of Particles, vol. 1, Cambridge University Press, 1995, p. 39, Eq. 3.4.
[26] J. Yang, Y. Huang, X. Wang, X.-B. Wang, F.F. Becker, P.R.C. Gascoyne, Dielectric properties of human leukocyte subpopulations determined by electrorotation as a cell separation criterion, Biophys. J. 76 (1999) 3307–3314.
[27] E.G. Cen, C. Dalton, Y. Li, S. Adamia, L.M. Pilarski, K.V.I.S. Kaler, A combined dielectrophoresis, traveling wave dielectrophoresis and electrorotation microchip for the manipulation and characterization of human malignant cells, J. Microbiol. Methods 58 (2004) 387–401.
[28] M. Madou, Fundamentals of Microfabrication, CRC-Press, Boca Raton, FL, 1998.
[29] V.L. Sukhorukov, W.M. Arnold, U. Zimmermann, Hypotonically induced changes in the plasma membrane of cultured mammalian cells, J. Membr. Biol. 132 (1993) 27–40.
[30] U. Zimmermann, The effect of high intensity electric field pulses on eukaryotic cell membranes: Fundamentals and applications, in: U. Zimmermann, G.A. Neil (Eds.), Electromanipulation of Cells, CRC Press, Boca Raton, Florida, 1996.